Journal of Hydrology: Regional Studies 36 (2021) 100876

Contents lists available at ScienceDirect

Journal of Hydrology: Regional Studies

journal homepage: www.elsevier.com/locate/ejrh

Effect of ENSO modulation by decadal and multi-decadal climatic oscillations on contiguous United States streamflows

Sarmistha Singh [a,*], Ash Abebe [b], Puneet Srivastava [c], Indrajeet Chaubey [d]

[a] Civil Engineering Department, Indian Institute of Technology Palakkad, Nila Campus, Kanjikode, Kerala, 678623, India
[b] Department of Mathematics & Statistics, Auburn University, 221 Parker Hall, Auburn, AL, 36849, USA
[c] University of Maryland, College of Agriculture and Natural Resources, College Park, MD, 20742-3131, USA; Affiliate Professor, Biosystems Engineering Department, Auburn University, Auburn, AL, 36832, USA
[d] College of Agriculture, Health and Natural Resources, University of Connecticut, 1376 Storrs Rd., Storrs, CT, 06269, USA

ARTICLE INFO

Keywords:
Streamflow
PLS
JRFit
ENSO
PDO
AMO

ABSTRACT

Study Region: The contiguous United States (CONUS).
Study Focus: This study assesses the effects of the large-scale oceanic-atmospheric oscillations such as El Niño southern oscillation (ENSO), Atlantic Multidecadal Oscillation (AMO), North Atlantic Oscillation (NAO), and Pacific Decadal Oscillation (PDO) on streamflow levels. Two robust and powerful non-parametric procedures, namely, the Joint Rank Fit (JRFit) and the rank-based partial least squares regression are used to identify and quantify the strength and direction of teleconnections (individual analysis). Further, JRFit is used to model the interactive effects (coupled analysis) of ENSO with AMO/PDO/NAO cycles on streamflows.
New Hydrological Insights for the Region: Individual analysis results identified new significant ENSO, PDO, AMO and NAO tele-connections with streamflows across CONUS. PLS analysis showed a stronger AMO teleconnection with streamflows compared to other oscillations. The coupled analyses results were categorized into three groups based on the types of interactions of the ENSO phases. Type 1 interactions where a phase of ENSO is modulated by phases of decadal/multidecadal cycles, are seen across all (majority of) regions in CONUS. Interesting results were obtained for type 2 (type 3) interactions as the effects of ENSO phases were opposite (similar but enhanced), compared to individual analysis of ENSO, when associated with the phases of PDO/AMO/NAO. The results provide several new findings and useful information for forecasting of water resources in the CONUS region.

1. Introduction

El Niño Southern Oscillation (ENSO), centered in the equatorial pacific, is one of the most studied ocean-atmospheric phenomena of tropical air-sea interactions. Its tele-connections to climate variations in the contiguous US on inter-annual timescales (for a periodicity of 2–7 years) are well documented (Walker, 1923; Kousky et al., 1984; Ropelewski and Halpert, 1989; Diaz and Markgraf, 1992, 2000; Gershunov and Barnett, 1998; Dai and Wigley, 2000; Goodrich, 2007). Similar to ENSO, the Pacific Decadal Oscillation (PDO), Atlantic Multidecadal Oscillation (AMO) and North Atlantic Oscillation (NAO) are also large-scale oceanic-atmospheric phenomena responsible for warming or cooling of the Pacific and Atlantic Ocean, respectively; however, they oscillate at different

* Corresponding author at: Civil Engineering Department, Indian Institute of Technology Palakkad, Kerala, 678623, India.
E-mail address: sarmistha@iitpkd.ac.in (S. Singh).

https://doi.org/10.1016/j.ejrh.2021.100876
Received 8 December 2020; Received in revised form 15 July 2021; Accepted 20 July 2021
Available online 28 July 2021

periodicities (decadal to multi-decadal).

In the recent past studies have generated greater interest related ENSO and other decadal/multidecadal climate cycles such as PDO, NAO and AMO and their effect on meteorological and hydrological parameters (Tootle et al., 2005; Araghinejad et al., 2006; Johnson et al., 2013; Mitra et al., 2014; Singh et al., 2015, 2016; Tamaddun et al., 2019a, 2019b). Several studies have investigated the tele-connections between sea conditions in the Atlantic and Pacific Oceans sea surface temperatures with regional precipitation and streamflow (Chiew et al., 1998; Schmidt et al., 2001; Sen et al., 2004; Tootle and Piechota, 2004; Murgulet et al., 2017). Streamflows in the United States have shown significant tele-connections to ENSO (Chiew and McMahon, 2002; Dracup and Kahya, 1994; Hamlet and Lettenmaier, 1999; Johnson et al., 2013; Tamaddun et al., 2017a,), PDO (Hamlet and Lettenmaier, 1999; Singh et al., 2015; Tamaddun et al., 2017a,), AMO and NAO (Tootle and Piechota, 2006; Singh et al., 2015).

Recent research has focused on coupling of the interannual ENSO with other decadal/multidecadal climatic oscillations such as PDO, AMO and NAO. Studies have shown that PDO modulates the strength of ENSO teleconnections to precipitation and droughts (Cayan et al., 1998; Gershunov and Barnett, 1998; McCabe et al., 2004). Similarly, Enfield et al. (2001) evaluated the impact of AMO on precipitation and found that most of the US experiences below normal precipitation during AMO positive phase. Rajagopalan et al. (2000) studied the coupled interactions of ENSO with PDO and NAO on meteorological droughts using the Palmer drought severity index. Coupled studies have also been conducted with respect to streamflows at a regional scale in the United States (Hidalgo and Dracup, 2001; Rogers and Coleman, 2003; Johnson et al., 2013; Singh et al., 2015; Murgulet et al., 2017; Tamaddun et al., 2017a,). As these studies are regional in nature, they fail to provide information at a larger CONUS scale. It is important to consider the CONUS as a whole for the evaluation and not limit to regional scale in order to understand the effect of large-scale oscillations on contiguous hydrology. Therefore, a study by Tootle et al. (2005) showed significant modulation of ENSO behavior dependent on the phases of AMO and PDO throughout the CONUS. They indicated that ENSO phase streamflows in the CONUS are influenced by other decadal and multidecadal oscillations. However, the study used the non-parametric statistical Wilcoxon rank sum test (WRS) to infer the interaction between ENSO and other decadal/multidecadal climate cycles without directly modelling the interaction effect (interaction test). Also, Singh et al. (2018) showed that the WRS test fails to account for monthly and seasonal cluster correlations within the data which might indicate erroneous results. Further, the study also failed to quantify the magnitude of the modulation across different regions and/or climate zones in the CONUS. Apart from that the strength of teleconnections and scaling rate (change in streamflow with one standard deviation change in climate index) of ENSO, PDO, AMO and NAO towards streamflow variability across the regions in the contiguous United States have not been quantified.

The quantification of the modulation magnitude, scaling rate, teleconnection strength and interaction test would indicate/provide predictive ability that can be helpful in forecasting of streamflows and water resources availability in the CONUS (Singh et al., 2018). Therefore, in this study, we revisit the topic of large-scale ocean-atmospheric cycle modulations on US streamflows and performed a comprehensive investigation on the interactive effect of climatic oscillations (i.e., ENSO, NAO, PDO and AMO) on streamflows in the entire CONUS using robust and efficient statistical procedures. We tested and evaluated the interactions (interaction test) between ENSO and other large-scale oscillations by directly modelling the interaction using a non-parametric linear mixed effects (LME) model. We used a powerful statistical procedure called Joint Rank Fit (JRFit) (Kloke et al., 2009; Singh et al., 2018) to fit the mixed effects model, and estimate the individual and coupled effects of climatic oscillations on streamflow levels for different regions across the CONUS. The JRFit model is able to efficiently model the interaction of two climate phenomena and works well for cluster correlated datasets (Singh et al., 2018). Moreover, the strength of tele-connection and scaling rate between the ocean-atmospheric cycles and streamflow levels were also quantified using a non-parametric rank-based partial least square (PLS) regression analysis. We also perform false discovery rate (FDR) analysis to test for false discovery rates in multiple hypothesis testing (Benjamini and Hochberg, 1995). Overall, with the help of these statistical analysis we identify and highlight new modulations/interactions by classifying the interactions into three major types of interactions in the CONUS region that were missed in the earlier studies.

Further, this study is conducted over an extended period of historic data (compared to Tootle et al. (2005)) that is required to more accurately and comprehensively evaluate the effect of inter-decadal phenomena on hydrologic variables. With a greater number of stations, higher record of data, and a powerful statistical technique, this comprehensive study provides a holistic picture of the effect of ocean-atmospheric cycles on streamflow levels across different climate zones in CONUS (Karl and Koss, 1984), which greatly adds to the current knowledge. The outcomes of this study will be helpful in developing streamflow forecasting frameworks across the CONUS region which incorporate climate oscillation information. Incorporating the information from ocean-atmospheric phenomena such as ENSO, NAO, PDO and AMO into the forecaster's toolbox can greatly improve the lead time in streamflow forecasting (Tootle et al., 2005; Araghinejad et al., 2006).

2. Methodology

A robust and powerful nonparametric model-fitting procedure known as JRFit procedure (Kloke et al., 2009) is applied to test and quantify the individual impacts of the phases of ENSO, NAO, PDO and AMO on streamflows. Moreover, a rank-based PLS approach is introduced to estimate the strength and direction of teleconnection effect of ENSO, AMO, PDO and NAO on streamflow fluctuations. Interaction tests between ENSO and the other climatic oscillations are performed to evaluate the modulation by NAO, AMO and PDO of ENSO effects on streamflow.

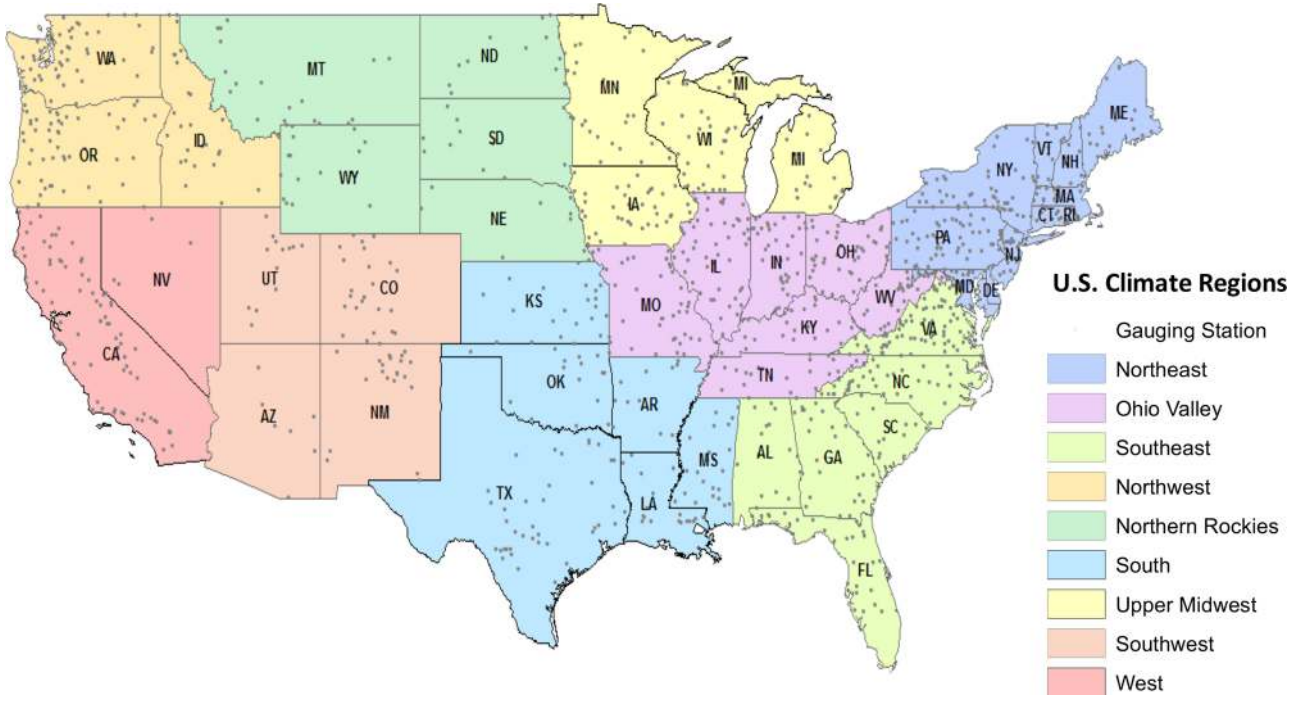

Fig. 1. This figure shows the nine climate regions within CONUS (modified from Karl and Koss, 1984). The gray dots show the location of the streamflow gauging stations.

2.1. Data

2.1.1. Streamflow data

The streamflow data were obtained from the Model Parameter Estimation Experiment (MOPEX) (Duan et al., 2006; Schaake et al., 2006). Since the spatial and temporal extent of the MOPEX data is large and do not have missing values, it is better suited for analysis related to decadal and multi-decadal climatic oscillations (Wang and Hejazi, 2011; Berghuijs et al., 2016). We extracted approximately 80 years (1920–2002) of daily streamflow data across the contiguous United States (Fig. 1) from MOPEX (Schaake et al., 2006) datasets, which are classified to be free of or minimally impacted by water management (Schaake et al., 2006). Monthly data were aggregated from daily data to evaluate the effects of climatic oscillations on streamflows.

2.1.2. Oceanic-atmospheric phenomena indicators

To identify teleconnections of climatic oscillations on streamflows, we used monthly PDO, ENSO, AMO and NAO indices from the "Joint Institute for the Study of the Atmosphere and Ocean, University of Washington" (Joint Institute for the Study of Atmosphere and Ocean (JISAO), 2012), "Climate Prediction Center (CPC) National Oceanic and Atmospheric Administration's (NOAA)", "Physical Sciences Division of the Earth Systems Research Laboratory, NOAA" (Earth Systems Research Laboratory (ESRL), 2012), and "National Center for Atmospheric Research (NCAR)", respectively. In this study, we used the Niño 3.4 SST index (ERSST.v3b) as the ENSO index. ENSO has three phases. Neutral phase is defined when Niño 3.4 index value is between -0.5 °C and +0.5 °C; El Niño (warm) and La Niña (cold) phases correspond to the values above +0.5 °C and below -0.5 °C, respectively. The phases of AMO and PDO (i.e., positive/warm and negative/cold) are defined based on positive and negative numerical values of SST anomalies (Table 1). The positive and negative phases of NAO are defined based on positive and negative numerical values of mean SLP anomalies (Table 1).

2.2. Statistical method

2.2.1. Joint rank fit (JRFit)

The nonparametric JRFit procedure extends the Wilcoxon rank-sum procedure to the estimation of mixed linear model parameters and their standard errors; therefore, it can be used for the analysis of models where the response variables exhibit cluster correlation (Kloke et al., 2009; Hettmansperger and McKean, 2011). In this study, the JRFit procedure was used to perform individual and coupled analyses. The Wilcoxon rank-sum procedure has long been used in hydrological studies (Tootle et al., 2005; Johnson et al., 2013,). This was extended by Jaeckel (1972) to the estimation of general linear models with independent responses and this procedure was extended to models with responses that are cluster correlated by Kloke et al. (2009). The new procedure, named JRFit, was shown to provide parameter estimators that are robust and efficient with an asymptotic normal distribution; hence, significance tests can be performed using Wald-type tests (Kloke et al., 2009).

Effects of individual ocean-atmospheric phenomena PDO, ENSO, NAO and AMO on streamflow were estimated using the simple linear model with binary regressor

$$\boldsymbol{S} = \boldsymbol{\beta}_0 + \boldsymbol{\beta}_1 \boldsymbol{X} + \boldsymbol{\varepsilon}, \tag{1}$$

where $\boldsymbol{S}$ represents the vector of streamflow values, $\boldsymbol{\varepsilon}$ represents a vector of unobserved random errors, and X represents a vector with $X = 0$ and $X = 1$ representing the positive/warm and negative/cold phases of the respective ocean-atmospheric oscillation. The magnitude of the slope coefficient β_1 is the amount by which streamflow changes when ocean-atmospheric oscillation changes phases. Cluster-correlation in streamflow data on a monthly basis means that the variance-covariance matrix of ε is block-diagonal where each block represents a month. JRFit provides an estimate of this matrix along with the regression coefficients. Note that in the case of independent responses, then (1) becomes a simple linear model and the test of the hypothesis $H : \beta_1 = 0$ via JRFit becomes the Wilcoxon rank-sum test (Hettmansperger and McKean, 2011).

Considering the Wilcoxon rank-sum test as a test of linear model parameters opens doors to studying more complicated effects of ocean-atmospheric oscillations. For instance, we can study the interactive effects of ocean-atmospheric oscillations on streamflow levels. The statistical model for the interaction (coupled) effects of ENSO with other climate oscillations on streamflows was

$$S = \beta_0 + \beta_1 X_1 + \beta_2 X_2 + \beta_3 (X_1 \odot X_2) + \ \varepsilon, \tag{2}$$

Table 1
The years classified as positive and negative phases of AMO, PDO, and NAO.

Climatic Oscillation Phases	AMO	PDO	NAO
Positive	1928– 1963, 1995– 2010	1925– 1944, 1977– 1999	1920– 1930 1941– 1951, 1973– 1976, 1981–2007
Negative	1920– 1927 1964– 1994	1920– 1924, 1945– 1976, 2000– 2010	1931– 1942 1952– 1972, 1977– 1980, 2008– 2010

where, X_1 entries are 0 for La Niña phase and 1 for El Niño phase, X_2 entries are 0 or Negative phase of PDO/NAO/AMO and 1 for Positive phase of PDO/NAO/AMO, and $X_1 \odot X_2$ is the component-wise product of X_1 and X_2. Thus β_3 estimates the interactive effect of ENSO with other ocean-atmospheric phenomena. The significance of the interaction coefficient β_3 represents the mitigation or enhancement of the effect of El Niño/La Niña on streamflow due to change of phases of the other climatic oscillations under consideration.

2.2.2. Robust partial least squares

Generally, partial least squares regression is the combination of principal component analysis and multiple regression. It proceeds by extracting orthogonal latent variables from the predictor variables possessing optimal fit to the response. Computation of PLS was facilitated by the statistically inspired modification of PLS (SIMPLS) algorithm (de Jong, 1993) and PLS can be constructed by their respective weight vectors or loadings w_k and orthogonal components or scores $t_k = Xw_k$ (Boulesteix and Strimmer, 2007) such that w_k maximizes $cov(t_k, Y)$. PLS's X components explain variance in Y with sequentially decreasing covariation.

PLS is sensitive to outliers, hence estimation of robust PLS scores was important in this study. In this research, we used a rank-based PLS score estimation introduced in Schneid (2015). This approach proceeds by replacing the covariance matrix in SIMPLS computation by a robust covariance matrix based on ranks. Note that $cov(t_k, Y) = var(t_k)var(Y)\rho_{tY}$, where ρ_{tY} is the Pearson product moment correlation between the scores t_k and response Y. The approach proposed by Schneid (2015) replaces ρ_{tY} by Spearman's rank correlation coefficient ρ^S_{tY} defined as

$$\rho^S_{tY} = corr(rank(t_k),\ rank(Y)) \tag{3}$$

Other proposed robust estimators of PLS scores also use SIMPLS and a robust covariance matrix estimated by a low-dimensional projection of the data [X,Y] via a robust algorithm of principal component analysis (Hubert and Branden, 2003). However, most of these procedures require complex computational algorithms (Møller et al., 2005; Kruger et al., 2008; González et al., 2009). The rank-based approach using bivariate Spearman's correlation estimates as a simple alternative for the robust covariance estimators is a simple approach that results in outlier-resistant PLS (Gil and Romera, 1998; Møller et al., 2005; Serneels et al., 2005; Rousseeuw et al., 2006; Daszykowski et al., 2007).

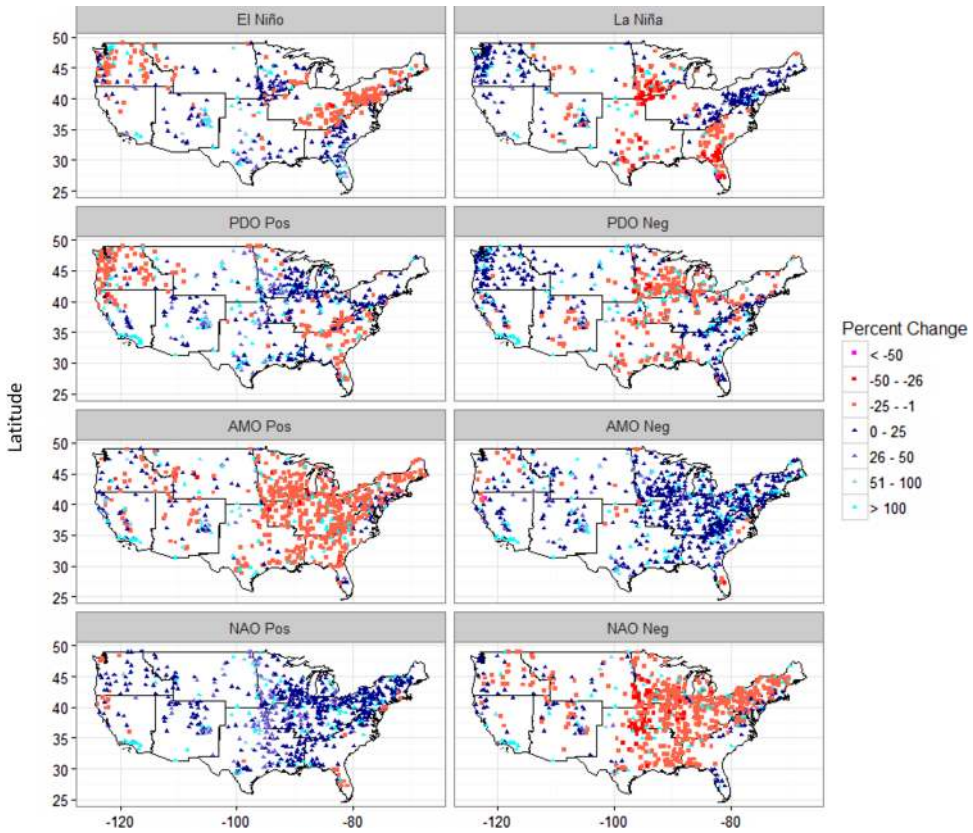

Fig. 2. Stations showing significant (90 %) difference in streamflow medians and percent increase/decrease in streamflows across all climate regions for different phases of ENSO, PDO, AMO, and NAO.

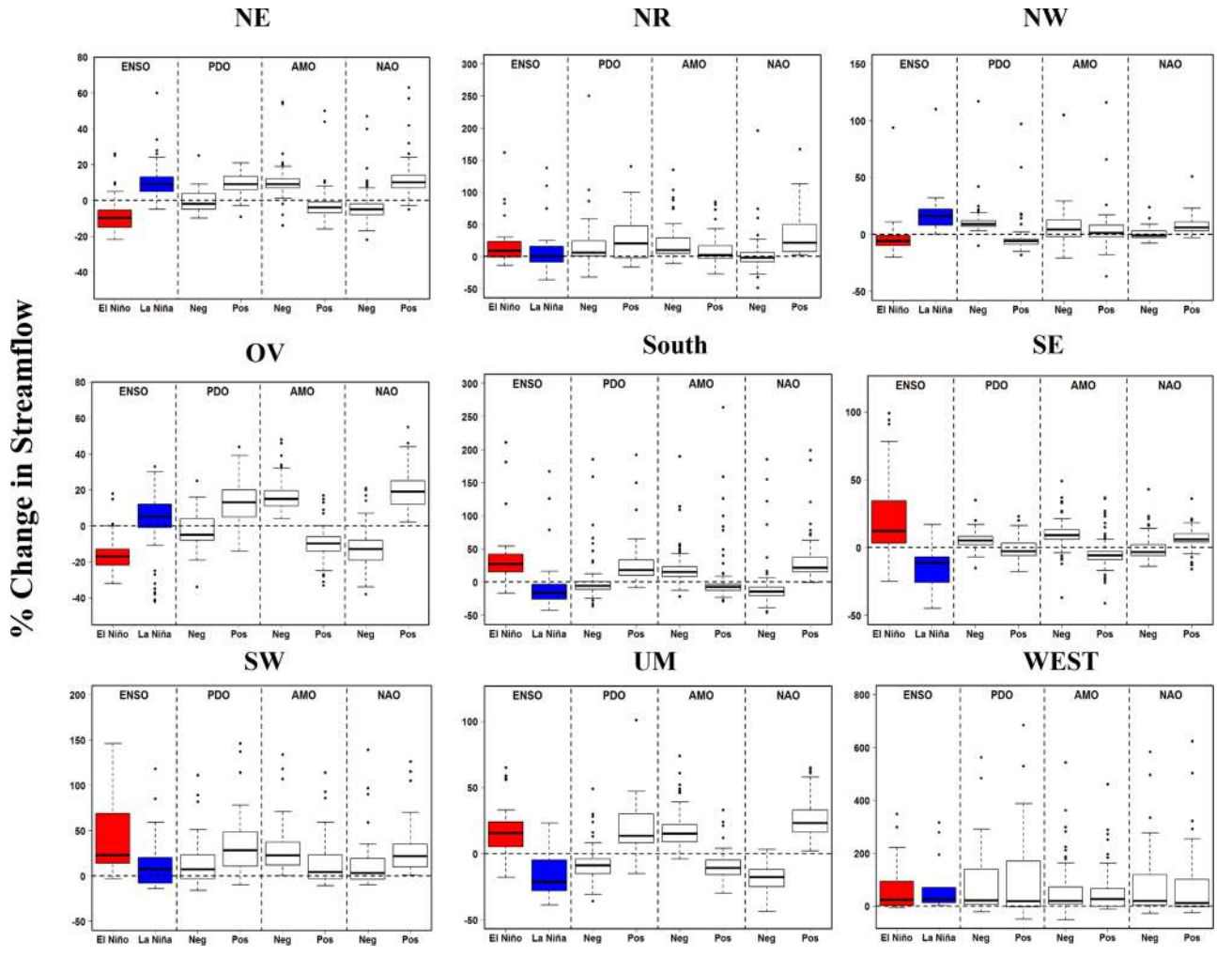

Fig. 3. Box and whisker plots of percent increase/decrease in streamflows medians compared to the long term medians for different climate regions due to individual effects of ENSO, PDO, AMO and NAO. The red and blue box plots represent El Niño and La Niña, respectively.

2.2.3. False discovery rate correction

Since we make station by station tests of hypotheses, we applied a false discovery rate correction using the step-up FDR procedure of Benjamini and Hochberg (1995) to control the proportion of hypotheses that are falsely declared significant. This is a common approach utilized when a large number of statistical tests are performed simultaneously and less stringent than family-wise error rate controlling methods such as the Bonferroni. Significance cutoff for FDR corrected p-values is often chosen higher than 0.05 (McDonald, 2009).

3. Results and discussion

3.1. Individual analysis

The results from the non-parametric JRFit procedure (Eq. (1)) for ENSO, PDO, AMO and NAO cycle are presented in Figs. 2 and 3. Following an FDR correction for multiple comparisons, the significant stations ($p < 0.10$) with the percentage change in estimated median streamflow for the phases of ENSO, AMO, PDO and NAO compared to the respective station long term medians are presented in Fig. 2. The comparison box and whisker plots showing the percentage change in median streamflows during the phases of ENSO, AMO, PDO and NAO for the nine climatic regions in the US is provided in Fig. 3. Moreover, the results from the non-parametric PLS analyses for all the climatic oscillations are presented in Figs. 4 and 5. PLS coefficients indicating the strength and direction of the tele-connections of ENSO, PDO, NAO and AMO cycles towards streamflow variability are provided in Fig. 4. Fig. 5 depicts similar information as Fig. 4; however, it presents the range of PLS coefficients for different regions. We also report the scaling rates for different cycle i.e., the estimated effect (in m^3/s) on regional median streamflow at one standard deviation change in the ENSO, PDO, AMO and NAO indices (Table 2).

3.1.1. ENSO

The JRFit results for ENSO indicate that all phases show significant teleconnection at all climatic regions except West and NR (Fig. 2). The results are consistent with well-established relationships of ENSO effects on streamflow levels in the Southeast (Schmidt et al., 2001; Tootle et al., 2005; Johnson et al., 2013; Singh et al., 2015) and Northwest US (Harshburger et al., 2002; Beebee and Manga, 2004). In the Southeast, El Niño/La Niña phases resulted in above/below normal streamflows while in the Northwest El Niño/La Niña phases led to below/above normal streamflows. Apart from these well-established findings, we also identified significant ENSO tele-connections with streamflows in NE, UM, South and the lower regions of OV (Fig. 2). The stations in NW, NE and lower OV showed decreased/increased streamflows during El Niño/La Niña phases while in the South and Midwest regions El Niño/La Niña phases resulted in higher/lower than normal streamflows (Fig. 3). Streamflow levels in NE, NW and OV were higher by approximately 10 %, 15 % and 8% (compared to long term median) (Fig. 3) during La Niña conditions, while for South, SE and UM the streamflow levels were lower by 20 %, 10 % and 25 % (compared to long term median), respectively (Fig. 3).

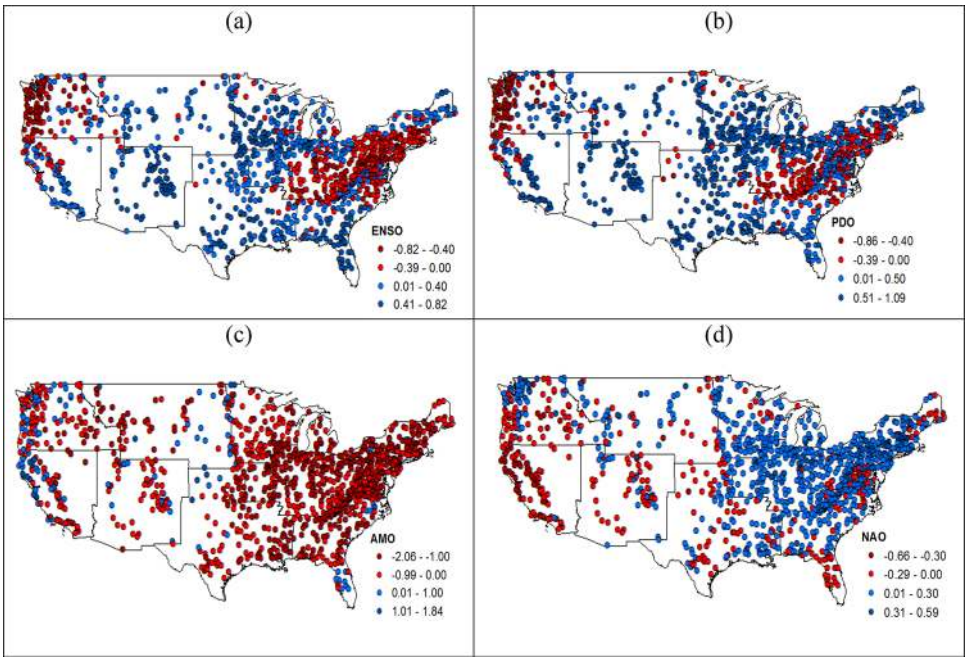

Fig. 4. Partial least square regression analysis coefficients indicating the strength and direction of teleconnections of (a) ENSO, (b) PDO, (c) AMO, and (d) NAO with streamflow.

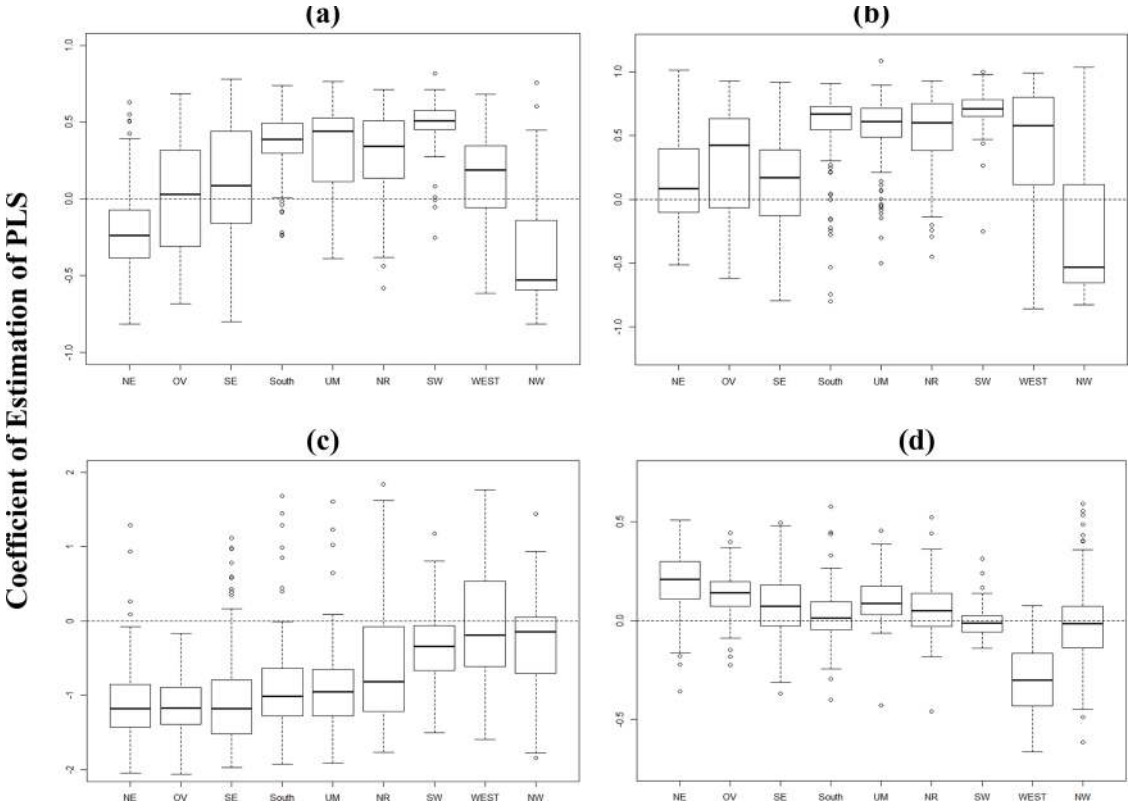

Fig. 5. Box and whisker plots showing the range of PLS coefficients indicating the strength and direction of teleconnections of (a) ENSO, (b) PDO, (c) AMO and (d) NAO with streamflow for all the climate regions in CONUS.

Table 2
Change in regional averaged monthly streamflow levels (m^3/s) with one standard deviation change in SSTs of ENSO, PDO, AMO, and NAO.

Index	ENSO	PDO	AMO	NAO
One Standard Deviation	0.8	1.11	0.14	1.04
Region	Change in Regional Averaged Streamflow (m^3/s)			
Northeast	−1.41	0.49	−6.98	1.24
Southeast	0.82	1.63	−11.15	0.68
South	5.23	9.05	−13.65	0.18
Southwest	1.70	2.37	−1.13	−0.04
Upper Midwest	4.29	5.96	−9.27	0.84
West	0.95	2.94	−0.95	−1.52
North Rockies	1.98	3.48	−4.70	0.29
North West	−7.47	−7.52	−2.04	−0.22
Ohio Valley	0.40	6.05	−16.77	2.02

The results from PLS regression analysis shows that the PLS coefficient (for ENSO index) is highly positive, indicating a strong positive teleconnection on streamflow levels, (i.e. streamflows increase with increase in ENSO SST) for all regions in CONUS except NE, NW, and in some parts of OV (Fig. 4 (a) and5) where major negative tele-connections were found (Fig. 4 (a) and 5). From Fig. 5 it is also evident that some stations in upper regions of SE also showed positive correlations with ENSO (Fig. 4 (a) and5). Moreover, the PLS analysis also quantified the overall scaling rate of ENSO on streamflow levels across different regions in CONUS (Table 2). Results show that one standard deviation increase in the ENSO index (0.8) resulted in an estimated regional median streamflow changes (from long term median) ranging from a drop of 7.47 m^3/s in NW to an increase of 5.23 m^3/s in the South (Table 2).

3.1.2. PDO

The PDO analysis identified climatic regions (NW, UM, OV, SE and S) where PDO showed prominent teleconnections (Figs. 2 and 3). Nigam et al. (1999) and Tootle et al. (2005) linked PDO tele-connections to the UM while Beebee and Manga (2004), and Tootle et al. (2005) indicated a PDO signal on Pacific Northwest streamflows. However, in this study we also identified stations in other climatic regions viz. South, lower regions in OV and SE which indicated statistically significant tele-connections with PDO. This

difference in results could be attributed to longer period of record and use of powerful non-parametric approach in this study. In NW and SE, positive/negative phases of PDO resulted in decrease/increase in streamflows, while the opposite was true for SW, UM, S and OV (Figs. 2 and 3). For the NW and SE climatic regions, streamflow levels were 8% lower (compared to long term medians) during the PDO positive phase while being 10 % and 8% higher (compared to long term medians) respectively, during the PDO negative phase.

The results from PLS regression analysis shows that the PLS coefficient (for PDO index) is highly positive, indicating a strong positive teleconnection on streamflow levels (i.e., streamflows increase with increase in PDO SST), for all regions in CONUS except NW, NE, northern regions of SE and in lower parts of OV (Figs. 4 (b) and5) where strong negative tele-connections were found (Fig. 4 (b) and5). Results on scaling rate show that one standard deviation increase in the PDO index (1.11) resulted in an estimated regional median streamflow changes ranging from a drop of 7.52 m^3/s for NW region and to an increase of 9.05 m^3/s for the South (Table 2).

3.1.3. AMO

The AMO analysis identified significant tele-connections across CONUS, with particularly stronger tele-connections along the east coast of the US (Fig. 4). The study conducted by Tootle et al. (2005) identified negative streamflow correlations with AMO phases in the upper to middle Mississippi River basin, lower Appalachians/Gulf of Mexico, and Southwest while identifying positive streamflow correlation in the Northwest. However, the results of this study indicate a wider range of tele-connections across the CONUS. The streamflow levels were below/above normal during the positive/negative phase of AMO in SE, NE, S, OV and UM climatic regions while it was above normal in the NR, SW, NW and West irrespective of phases of AMO (Figs. 2, 3 and 4).

A study conducted by Enfield et al. (2001) also correlated the AMO phases with precipitation across the US and identified that precipitation exhibited significant negative correlations with AMO phases throughout the US, except for in the Pacific Northwest. Negative AMO phase streamflows were approximately 20 % higher compared to the long-term medians across all the climate regions, while streamflow levels decreased by approximately 10 % (compared to long term medians) during the positive phase for NE, OV, South, SE, and UM regions (Fig. 3). The PLS analysis results also showed that PLS coefficient (for PDO index) is highly negative for most of the regions in CONUS (Fig. 4(b)). Results on scaling rates show that one standard deviation (0.14) increase in AMO index leads to estimated regional median streamflow changes ranging from a drop of 16.77 m^3/s in OV to an increase of 0.95 m^3/s in the West

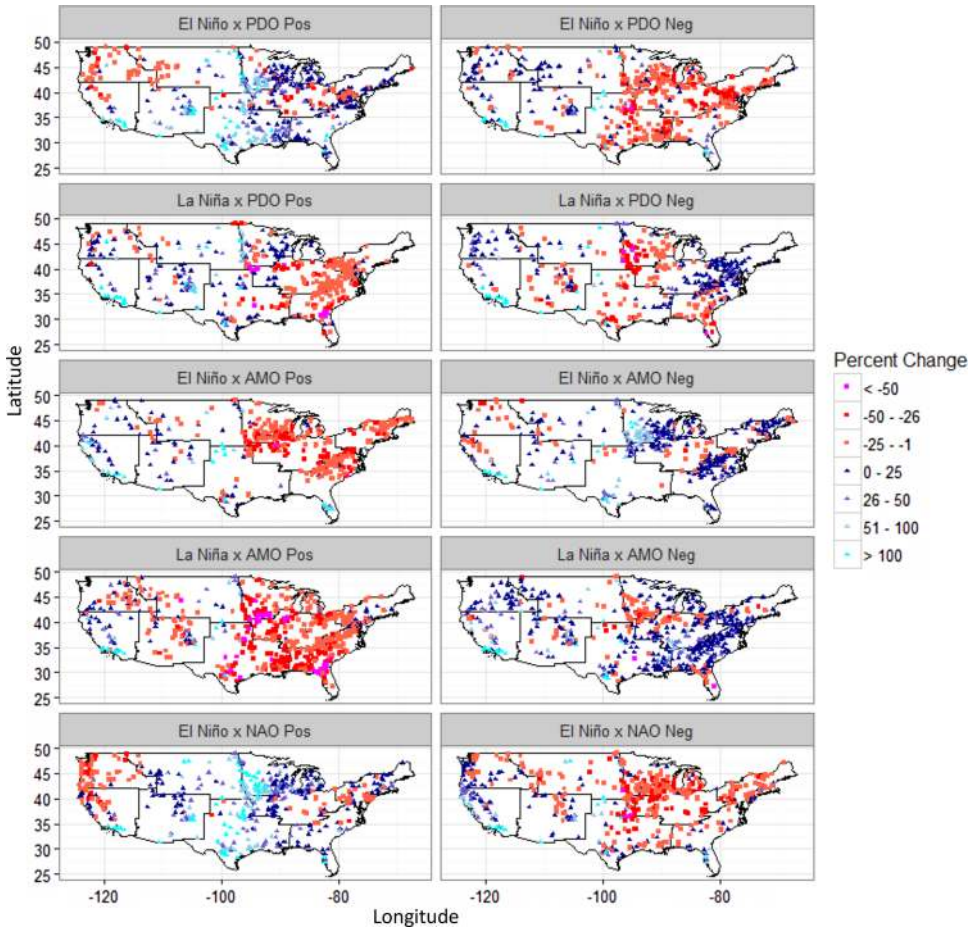

Fig. 6. Stations showing significant (at 90 %) stations and the percent change in median streamflows for El Niño and La Niña phases associated with positive (Pos) and negative (Neg) phases of PDO, AMO and NAO.

(Table 2). It is important to note that the PLS coefficients and scaling rates for AMO are negative for all the regions with higher magnitudes compared to ENSO, PDO and NAO, highlighting the strong negative teleconnection of AMO with streamflows across the CONUS (Fig. 4 and Table 2).

3.1.4. NAO

Streamflow generally increased during NAO positive phases showing an average increase of approximately 20 % (compared to long term medians) across all the climate regions, except the West (Fig. 2 and 3). Significant differences in streamflows were found in four distinct regions i.e., the NE, OV, South and UM where most of the stations showed below normal streamflows (approximately 10 %–25 %) during the NAO negative phase (Fig. 3). Tootle et al. (2005) found significant differences between the phases of NAO and observed an increase streamflows during the positive phase than negative phase of NAO in the upper to middle Mississippi River basin (UM and OV) only. Visbeck et al. (2001) also identified significant correlations in NE. The results from this study validate some of the results from the previous studies, however the results from the current research also identified strong teleconnections in other climatic regions viz. SE, S, NR and NW. The streamflow levels of these regions increased by approximately 8–25 % (compared to long term medians) during the NAO positive phase and decreased by 5–12 % during the negative phase.

Moreover, the results from PLS regression analysis also asserts that NAO has positive teleconnections with streamflows across all the climatic regions except West (Fig. 4 and 5). It was also found that the overall strength of teleconnection of NAO on streamflows in CONUS was the least among the other climatic oscillations (Fig. 4). An increase of one standard deviation (1.04) in the NAO index leads to estimated regional median streamflow changes ranging from a drop of 1.52 m^3/s in the West to an increase of 2.02 m^3/s in OV region (Table 2).

3.2. Coupled analyses

The JRFit estimate of interaction term in the linear mixed effect model (Eq. 2) was used to measure the coupled effects of ENSO with PDO, NAO and AMO on streamflow. Subsequently, the FDR correction was applied to the interaction test. Significant ($p < 0.10$) interaction between ENSO and any other climate cycles (for example PDO) is an indicator of unequal modulation of the phases of ENSO by negative and positive phases of that cycle (for example PDO). Following a significant interaction test, simple-main effect comparisons were performed by comparing the phases of PDO, AMO, and NAO with each phase of ENSO using JRFit. Stations that showed significant interactions following an FDR correction ($p < 0.10$) were identified and the percent differences of El Niño and La Niña streamflow medians (from the station median) when coupled with the phases of PDO, AMO, and NAO are presented in Fig. 6. Fig. 7 gives the percent differences of streamflow medians (from long term station medians) for El Niño and La Niña phases coupled with the positive and negative phases of PDO, AMO, and NAO (including non-significant stations). Broadly, all climate regions exhibited significant coupled effects of ENSO and PDO as well as ENSO and AMO on streamflow. Moreover, the interaction effect of ENSO and NAO was significant across all the climate regions except in the Southeast where only a few stations were found to be significant. Due to the different types of interactions observed between decadal/multidecadal cycles (either AMO/PDO/NAO) and ENSO, we categorize

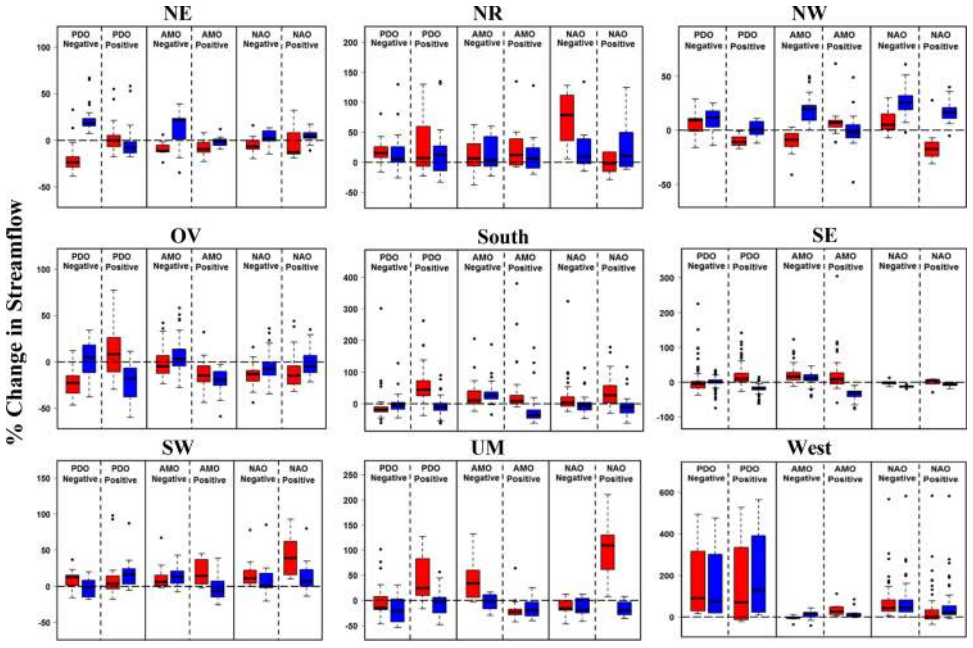

Fig. 7. Box and whisker plots of the percentage change in median streamflows (compared to long term medians) for El Niño (red) and La Niña (blue) phases associated with positive and negative phases of PDO, AMO, and NAO across all the climate regions.

the results in three major interaction types:

Interaction Type 1: Positive and negative phases of decadal/multidecadal cycles (AMO/PDO/NAO) are responsible for modulation of either phases of ENSO. Type 1 interaction are further subdivided into two types:

- Type 1A Interaction: when positive and negative phases of decadal/multidecadal cycles (AMO/PDO/NAO) modulates El Niño phases only.
- Type 1B Interaction: when positive and negative phases of decadal/multidecadal cycles (AMO/PDO/NAO) modulates La Niña phases only.

Type 2 Interaction: A phase of decadal/multidecadal cycle (AMO/PDO/NAO) modulates either/both the phases of ENSO, such that the sign of "percentage streamflow change" values for either/both the phases of ENSO flip compared to the ENSO individual analysis.

Type 3 Interaction: A phase of decadal/multidecadal cycle (AMO/PDO/NAO) modulates either/both the phases of ENSO, such that the magnitude of "streamflow change values" for either/both the phase of ENSO shifts considerably (without flipping the sign) compared to the ENSO individual analysis (however the sign does not change).

It is important to note that the interaction Type 1 and Type 2/3 are not mutually exclusive i.e., Type 1 can occur simultaneously with Type 2 or Type 3. While Type 2 and Type 3 interactions are by definition mutually exclusive.

3.2.1. ENSO and PDO

For the ENSO-PDO analysis, Type 1 interactions are seen across almost all regions in CONUS. Strong influence of PDO negative and positive phases were observed on La Niña and El Niño streamflows, respectively across the CONUS. The most significant combinations are that of La Niña associated PDO negative phase and El Niño associated PDO positive phase which exhibited above normal streamflow in the NW and SE, respectively. This is consistent with the findings of Gershunov and Barnett (1998) that PDO has strong influence on ENSO for sea level pressures and heavy daily precipitation in the contiguous United States and El Niño (La Niña) signals were found to be strong and stable during the positive (negative) PDO phase. Tootle et al. (2005) identified that PDO influence El Niño streamflows in the upper to middle Mississippi River basin only (at higher significance level) where the phases of PDO influence El Niño streamflow however, but they failed to identify PDO-ENSO interaction for the rest of the US. In this study, due to the introduction of JRFit interactive test, the ENSO-PDO interaction on streamflow levels was found to be significant across other climatic regions as well.

Strong significant differences were observed in El Niño streamflows when associated with PDO positive and negative phases for the entire CONUS except for the SW, West and NR (Fig. 6; Type 1A). Similarly, significant differences were observed in La Niña streamflows when coupled with PDO negative and positive phases except for the South and NR regions (Fig. 6; Type 1B*)*. La Niña coupled with positive phases of PDO resulted in 25 % decrease in streamflow in the SE linked with extreme droughts in this region during these periods (Fig. 7). However, La Niña associated with the positive phase of PDO resulted in approximately 25 % and 100 % increase in streamflow in the SW and West, respectively, compared to overall La Niña phases (Fig. 7).

Type 2 interactions are also seen in the ENSO-PDO interaction analysis. Contrary to ENSO individual analysis, it was found that for positive phase PDO, streamflow levels were higher during the El Niño phase and lower during the La Niña phase for the NE and OV (Fig. 6 and 7). Similar Type 2 interactions also suggest that El Niño is modulated by the negative phase of PDO in the NW, UM, South and SE. The percent changes in median streamflow levels were above normal during El Niño phase associated with PDO negative phase for NW (contrary to ENSO individual analysis). Also, El Niño phase streamflows were below normal (approximately 25 %) during PDO negative phase for the UM, South and SE, also contrary to the results of the ENSO individual analyses (Figs. 6 and 7). These results derived from interaction tests, clearly provides new insights on how the ENSO phases are modulated by the phases of PDO across CONUS that are contrary to the findings of individual analysis and have not reported in earlier literature studies (Tootle et al., 2005; Johnson et al., 2013; Bhandari et al., 2018; Tamaddun et al., 2017a, 2019). These findings also indicate that individual analysis results can sometimes be disinforming if not considered in conjunction of the interaction effects of other decadal/multidecadal cycles.

3.2.2. ENSO and AMO

Interaction of ENSO streamflows due to AMO cycles were observed at almost all regions in the CONUS. Several researchers have identified this modulation effect for SE (Tootle et al., 2005 and Singh et al., 2015), however, in this study we found that the modulation effect exists for other regions in CONUS as well. Type 1 interactions were observed in NW, UM, OV, NR and West regions. Type 1A interactions were observed in the NW, UM and OV where highly significant differences in El Niño streamflows when associated with AMO positive and negative phases (Fig. 6). Similarly, Type 1B interactions were observed in entire CONUS region (with the exception of NR, UM and West) where significant differences were observed in La Niña streamflows when associated with AMO positive and negative phases.

Type 2 interaction were observed in some parts of CONUS as well. Contrary to the results in ENSO individual analysis, La Niña events occurring in an AMO positive phase result in decreased streamflow in the NE, OV and SW. This indicates that La Niña does not always cause wetter conditions in these regions, rather when associated with AMO positive phase can lead to drier conditions in these regions. Similarly Type 2 interactions were also observed in South and SE regions. Significant differences in La Niña streamflow levels were observed in these regions when associated with the positive and negative phases of AMO. As per individual ENSO analysis, La Niña events lead to decreased streamflow levels in the South and SE (Figs. 6), however La Niña events coinciding with the AMO negative phase result in above normal streamflow levels countering La Niña's negative effect on streamflows in this region.

Type 3 interaction was also observed in the AMO-ENSO analysis. La Niña coupled with AMO positive resulted in significantly

greater reduction (approximately 35 %) in streamflow than individual La Niña phase (Fig. 7) leading to severe droughts in the SE and South regions. Moreover, the percentage changes in median streamflows were above normal (approximately 15 %) and below normal (approximately 25 %) during El Niño-AMO positive phase in NW and UM, respectively, compared to individual El Niño phase (Fig. 7).

3.2.3. ENSO and NAO

For ENSO-NAO, a significant association was seen for El Niño with NAO phases in UM, NW and NR regions, however La Niña association with NAO phases were not significant in the CONUS region. From the individual analysis it was found that an El Niño phase usually led to an increased streamflow in the UM however, when coinciding with NAO negative phase (Figs. 6 and 7), resulted in below normal streamflow (Type 2 interaction). This result asserts the findings from Tootle et al., 2005. However, in this study, different interactions with respect to ENSO-NAO were also observed. El Niño associated with the positive phase of NAO resulted in greater increase in streamflow (approximately 100 %) in the UM suggesting a modulation effect of both phases of NAO on El Niño streamflow levels (Type 1A interaction).

In NR region, El Niño during NAO negative phase resulted in greater increase in streamflow compared to individual ENSO (approximately 80 %; Type 3 interaction) (Fig. 7). Higher than normal streamflows were identified in NW during the El Niño phase occurring in an NAO negative phase which differs from the ENSO individual analysis where streamflow levels were below normal during El Niño phases (Type 2 interaction). Moreover, El Niño phase occurring in an NAO positive phase resulted in a greater decrease in streamflow levels (approximately 20 %) as compared to individual El Niño results (approximately 5%; Type 3 interaction).

4. Conclusions

This study systematically investigates the relationships between interdecadal and interannual ocean-atmospheric phenomena on streamflow levels across nine climate regions of the CONUS. This research made a number of novel contributions towards the understanding of the interplay between large-scale interannual and multidecadal ocean-atmospheric oscillations and its connection to CONUS streamflow levels using powerful and robust statistical procedures. Previous studies used common statistical procedures (viz. wavelet analysis and WRS) to detect teleconnections and infer the interaction between ENSO and other decadal and multi-decadal climate cycles without performing interaction test (Tootle et al., 2005; Johnson et al., 2013; Mitra et al., 2014; Bhandari et al., 2018; Tamaddun et al., 2019a). However, in this study we model the interactions using the interaction test to identify newer interactions that were not reported in earlier literature. We tested and evaluated the interactions (interaction test) between ENSO and other large-scale oscillations by directly modelling the interaction using a non-parametric LME model. We also used a powerful statistical procedure (JRFit) to fit the mixed effects model and estimate the individual and coupled effects of climatic oscillations on streamflow levels. Further we quantify the magnitude of the modulation, scaling rates, teleconnection strength across climate zones in the CONUS. The entire study was divided into individual and coupled analysis.

The major and new findings in the individual analysis are summarized below:

1 In the individual ENSO analysis almost all the regions showed significant tele-connections. In this study several new tele-connections were also identified viz. in NE, UM, West, South and the lower regions of OV.
2 In PDO individual analysis several regions were identified having tele-connections with PDO. However, in this study, South, lower regions in OV and SE also indicated statistically significant teleconnections with PDO, that were not reported in earlier literature.
3 The negative correlation of AMO with streamflow was apparent across climate regions, however some new areas exhibiting significant positive correlation (where streamflow increased during positive AMO phase) were identified in the West and some parts of Northwest, NR and SW.
4 The effect of NAO on streamflow levels was found to be positive across all the climatic regions except West, SW and NW regions where streamflow decreased during NAO negative phase. Newer tele-connections were observed in SE, S, NR and NW.
5 The PLS coefficients and scaling rates for AMO highlight the strong negative tele-connection of AMO with streamflows across the CONUS (compared to ENSO, PDO and NAO).

Coupled analysis reveal the interplay between large scale interannual and decadal variations in climate (e.g., the relationship between the ENSO with PDO, AMO and NAO), which may modulate the teleconnections with streamflow in CONUS region. The study presented here contributes to an improved understanding of how interdecadal phenomena modulate the effect of ENSO and its impact on streamflow levels in the nine climate regions across the US. Through interaction test between ENSO with AMO, PDO and NAO, three types of interaction results were identified.

Some of the major and newer findings in the coupled analysis are summarized below:

1 Significant Type 1 ENSO-PDO interactions are seen across all regions in CONUS. Such interactions were also observed for ENSO-AMO at majority of the regions in CONUS (NW, UM, OV, NR, UM and West).
2 Type 2 interactions discovered in this study were interesting as they generally go against the results of ENSO individual analysis. For example, contrary to the results in ENSO individual analysis, La Niña events occurring in an AMO positive phase result in decreased streamflow in the NE, OV and SW. This indicates that La Niña does not always cause wetter conditions in these regions, rather when associated with AMO positive phase can lead to drier conditions in these regions. Similar Type 2 interactions were found for all ENSO-PDO, ENSO-AMO and ENSO-NAO coupled analysis.

3 Type 3 interactions involve where the results of the ENSO individual analysis are enhanced due to the interaction of the phases of ENSO with other cycles. For example, La Niña coupled with AMO positive resulted in significantly greater reduction (approximately 35 %) in streamflow than individual La Niña phase. Prominent Type 3 interactions were observed with ENSO-AMO analysis in the SE and south regions. Moreover, in ENSO-NAO analysis Type 3 interactions were observed in NW and NR regions.

The results from this study will be helpful in development of better forecasting tools. Studies have shown that incorporating large-scale climate information could lead us to more accurate (specificity) hydrological forecasts with increase in the lead times signals (Grantz et al., 2005; Abrishamchi et al., 2006; Singh, 2016). This current research will help provide important information to water managers responsible for predicting streamflow variability in response to ocean atmospheric oscillations in CONUS. It would also help regional water managers in forecasting regional water availability, hydropower generation, and help them develop drought adaptation and mitigation strategies by incorporating information based on the large-scale ocean-atmospheric cycles.

It is however important to note that the entire analysis is based on non-parametric statistics that is primarily data driven and does not consider the physical processes involved in modelling the modulation/interaction effect. Therefore, model-based studies are needed to validate the findings of this study. Moreover, the record length of 80 years of streamflow data is still limited when considering the analysis with respect to multidecadal cycles as very only few phases of each cycle can be considered (especially for modelling interactions), limiting the robustness of the results.

Code availability

The R codes used in this study can be made available by writing to the corresponding author.

Data availability

The hydrological data sets used in this study are available at the “Model Parameter Estimation Experiment (MOPEX)”, “NOAA’s National Weather Services”. ENSO (Niño 3.4) SST index is available at “Climate Prediction Center (CPC), NOAA’s National Weather Services”. Similarly, PDO, NAO and AMO indices data can be obtained from “Joint Institute for the Study of the Atmosphere and Ocean, University of Washington (Joint Institute for the Study of Atmosphere and Ocean (JISAO), 2012)”, “National Center for Atmospheric Research (NCAR)”, and “Physical Sciences Division of the Earth Systems Research Laboratory, NOAA (Earth Systems Research Laboratory (ESRL), 2012)”, respectively.

Author contribution

SS, AA and PS formulated the idea behind this study. SS and AA performed the analysis and wrote the paper. AA, PS and IC contributed towards editing the paper.

Declaration of Competing Interest

The authors declare that they have no conflict of interest.

Acknowledgments

The authors would like to acknowledge the National Integrated Drought Information System (NIDIS) and Alabama Agricultural Experiment Station (AAES) grant programs for providing the funding for this study. The authors would like to thank the Editor and the three anonymous reviewers for providing constructive suggestions to improve the quality of the paper.

Appendix A. Supplementary data

Supplementary material related to this article can be found, in the online version, at doi:https://doi.org/10.1016/j.ejrh.2021.100876.

References

Araghinejad, S., Burn, D.H., Karamouz, M., 2006. Long-lead probabilistic forecasting of streamflow using ocean-atmospheric and hydrological predictors. Water Resour. Res. 42, W03431 https://doi.org/10.1029/2004WR003853.

Benjamini, Y., Hochberg, Y., 1995. Controlling the false discovery rate: a practical and powerful approach to multiple testing. J. R. Stat. Soc. Ser. B 57 (1), 289–300.

Berghuijs, W.R., Woods, R.A., Hutton, C.J., Sivapalan, M., 2016. Dominant flood generating mechanisms across the United States. Geophys. Res. Lett. 43, 4382–4390.

Bhandari, S., Kalra, A., Tamaddun, K., Ahmad, S., 2018. Relationship between ocean-atmospheric climate variables and regional streamflow of the conterminous United States. Hydrology 5 (2). https://doi.org/10.3390/hydrology5020030.

Boulesteix, A.-L., Strimmer, K., 2007. Partial least squares: a versatile tool for the analysis of high-dimensional genomic data. Brief. Bioinformatics 8, 32–44.

Cayan, D.R., Dettinger, M.D., Diaz, H.F., Graham, N.E., 1998. Decadal variability of precipitation over western North America. J. Clim. 11, 3148–3166.

Chiew, F.H., McMahon, T.A., 2002. Global ENSO-streamflow teleconnection, streamflow forecasting and interannual variability. Hydrol. Sci. J. 47 (505), 522.
Chiew, F.H.S., Piechota, T.C., Dracup, J.A., McMahon, T.A., 1998. El Niño/Southern oscillation and Australian rainfall, streamflow and drought: links and potential for forecasting. J. Hydrol. 204, 138–149.
Dai, A., Wigley, T.M.L., 2000. Global patterns of ENSO-induced precipitation. Geophys. Res. Lett. 27, 1283–1286.
Daszykowski, M., Kaczmarek, K., Vander Heyden, Y., Walczak, B., 2007. Robust statistics in data analysis - a review: basic concepts. Chemom. Intell. Lab. Syst. 85, 203–219.
de Jong, S., 1993. SIMPLS: an alternative approach to partial least squares regression. Chemom. Intell. Lab. Syst. 18, 251–263.
Diaz, H.F., Markgraf, V., 1992. El Niño: Historical and Paleoclimatic Aspects of the Southern Oscillation. Cambridge University Press.
Diaz, H.F., Markgraf, V. (Eds.), 2000. El Niño and the Southern Oscillation.. Cambridge University Press, United Kingdom, 496pp.
Dracup, J.A., Kahya, E., 1994. The relationships between US streamflow and La Niña events. Water Resour. Res. 30, 2133–2141.
Duan, Q., et al., 2006. Model parameter estimation experiment (MOPEX): an overview of science strategy and major results from the second and third workshops. J. Hydrol. 320 (1), 3–17.
Earth Systems Research Laboratory (ESRL), 2012. Climate Timeseries: AMO (Atlantic Multidecadal Oscillation) Index. http://www.esrl.noaa.gov/psd/data/timeseries/AMO/.
Enfield, D.B., Mestas-Nuez, A.M., Trimble, P.J., 2001. The Atlantic multi-decadal oscillation and its relation to rainfall and river flows in the continental US. Geophys. Res. Lett. 28 (10), 2077–2080.
Gershunov, A., Barnett, T.P., 1998. Inter-decadal modulation of ENSO teleconnections. Bull. Am. Meteorol. Soc. 79, 2715–2725.
Gil, J.A., Romera, R., 1998. On robust partial least squares (PLS) methods. J. Chemom. 12, 365–378.
González, J., Pena, D., Romera, R., 2009. A robust partial least squares regression method with applications. J. Chemom. 23, 78–90.
Goodrich, G.B., 2007. Multidecadal climate variability and drought in the United States. Geogr. Compass 1.
Grantz, K., Rajagopalan, B., Clark, M., Zagona, E., 2005. A technique for incorporating large-scale climate information in basin-scale ensemble streamflow forecasts. Water Resour. Research 41, W10410.
Hamlet, A.F., Lettenmaier, D.P., 1999. Columbia River streamflow forecasting based on ENSO and PDO climate signals. J. Water Resour. Plann. Manage. 125, 333–341.
Hettmansperger, T.P., McKean, J.W., 2011. Robust Nonparametric Statistical Methods, Volume 119 of Monographs on Statistics and Applied Probability, second edition. CRC Press, Boca Raton, FL.
Hidalgo, H.G., Dracup, J.A., 2001. Evidence of the Signature of North Pacific Multidecadal Processes on Precipitation and Streamflow Variations in the Upper Colorado River Basin, Paper Presented at the 6th Biennial Conference of Research on the Colorado River Plateau. U.S. Geol. Surv., Phoenix, Ariz.
Hubert, M., Branden, K.V., 2003. Robust methods for partial least squares regression. J. Chemom. 17, 537–549.
Jaeckel, L.A., 1972. Estimating regression coefficients by minimizing the dispersion of the residuals. Ann. Math. Stat. 43, 1449–1458.
Johnson, N.T., Martinez, C.J., Kiker, G.A., Leitman, S., 2013. Pacific and Atlantic sea surface temperature influences on streamflow in the Apalachicola–Chattahoochee–Flint river basin. J. Hydrol. 489, 160–179.
Joint Institute for the Study of Atmosphere and Ocean (JISAO), 2012. PDO Index. http://jisao.washington.edu/pdo/PDO.latest.
Karl, T.R., Koss, W.J., 1984. Regional and national monthly, seasonal, and annual temperature weighted by Area, 1895-1983. Historical Climatology Series 4-3. National Climatic Data Center, Asheville, NC, p. 38.
Kloke, J.D., McKean, J.W., Rashid, M., 2009. Rank-based estimation and associated inferences for linear models with cluster correlated errors. J. Am. Stat. Assoc. 104 (485), 384–390.
Kousky, V.E., Kagano, M.T., Cavlcanti, I.F.A., 1984. A review of the Southern Oscillation: oceanic-atmospheric circulation changes and related rainfall anomalies. Tellus 490–502, 36A.
Kruger, U., Zhou, Y., Wang, X., Rooney, D., Thompson, J., 2008. Robust partial least squares regression: part I, algorithmic developments. J. Chemom. 22, 1–13.
McCabe, G.J., Palecki, M.A., Betancourt, J.L., 2004. Pacific and Atlantic Ocean influences on multidecadal drought frequency in the United States. In: Proceedings of the National Academy of Sciences, 101, pp. 4136–4141.
McDonald, J.H., 2009. Handbook of Biological Statistics, 2nd ed. Sparky House Publishing, Baltimore, Maryland.
Mitra, S., Srivastava, P., Singh, S., Yates, D., 2014. Effect of ENSO-Induced climate variability on groundwater levels in the Lower Apalachicola-Chattahoochee-Flint River Basin. Trans. Asabe 57 (5), 1393–1403.
Møller, S.F., von Frese, J., Bro, R., 2005. Robust methods for multivariate data analysis. J. Chemom. 19, 549–563.
Murgulet, D., Valeriu, M., Hay, R.R., Tissot, P., Mestas-Nuñez, A.M., 2017. Relationships between sea surface temperature anomalies in the Pacific and Atlantic Oceans and South Texas precipitation and streamflow variability. J. Hydrol. 550, 726–739.
Rajagopalan, B., Cook, E., Lall, U., Ray, B.K., 2000. Spatiotemporal variability of ENSO and SST teleconnections to summer drought over the United States during the twentieth century. J. Clim. 13 (4244), 4255.
Rogers, J.C., Coleman, J.S.M., 2003. Interactions between the Atlantic Multidecadal Oscillation, el Niño/La Niña, and the PNA in winter Mississippi Valley stream flow. Geophys. Res. Lett. 30 (10) https://doi.org/10.1029/2003GL017216, 1518.
Ropelewski, C., Halpert, M., 1989. Precipitation patterns associated with the high index phase of the Southern Oscillation. J. Clim. 2, 268–284.
Rousseeuw, P.J., Debruyne, M., Engelen, S., Hubert, M., 2006. Robustness and outlier detection in chemometrics. Crit. Rev. Anal. Chem. 36, 221–242.
Schaake, J., Cong, S., Duan, Q., 2006. U.S Mopex Datasets, IAHS Publication Series 20. https://ereports-ext.llnl.gov/pdf/333681.pdf).
Schmidt, N., Lipp, E.K., Rose, J.B., Luther, M.E., 2001. ENSO influences on seasonal rainfall and river discharge in Florida. J. Clim. 14, 615–628.
Sen, Z., Altunkaynak, A., Özger, M., 2004. El Niño Southern Oscillation (ENSO) templates and streamflow prediction. J. Hydrol. Eng. 9, 368–374.
Serneels, S., Croux, C., Filzmoser, P., Van Espen, P.J., 2005. Partial robust M-regression. Chemom. Intell. Lab. Syst. 79, 55–64.
Singh, S.K., 2016. Long-term streamflow forecasting based on ensemble streamflow prediction technique: a case study in New Zealand. Water Resour. Manag. 30, 2295–2309.
Singh, S., Srivastava, P., Abebe, A., Mitra, S., 2015. Baseflow response to climate variability induced droughts in the Apalachicola–Chattahoochee–Flint River Basin. U.S.A. Journal of Hydrology 528, 550–561.
Singh, S., Abebe, A., Srivastava, P., 2018. Evaluation of nonparametric and parametric statistical procedures for modelling and prediction of cluster-correlated hydroclimatic data. Water Resour. Res. 54, 6948–6964.
Tamaddun, K.A., Kalra, A., Ahmad, S., 2019a. Spatiotemporal variation in the continental US streamflow in association with large-scale climate signals across multiple spectral bands. Water Resour. Manag. 33 (6), 1947–1968.
Tamaddun, K.A., Kalra, A., Bernardez, M., Ahmad, S., 2019b. Effects of ENSO on temperature, precipitation, and potential evapotranspiration of north India's monsoon: an analysis of trend and entropy. Water 11 (2). https://doi.org/10.3390/w11020189.
Tootle, G.A., Piechota, T.C., 2004. Suwannee river long range streamflow forecasts based on seasonal climate predictors. J. Am. Water Resour. Assoc. 40, 523–532.
Tootle, G.A., Piechota, T.C., 2006. Relationships between Pacific and Atlantic Ocean Sea surface temperatures and US streamflow variability. Water Resour. Res. 42, 7411.
Tootle, G.A., Piechota, T.C., Singh, A., 2005. Coupled oceanic–atmospheric variability and US streamflow. Water Resour. Res. 41, 1–11.
Walker, G.T., 1923. Correlation in seasonal variations of weather. VIII. A preliminary study of world-weather. Memoirs Indian Meteorological Department 24 (Part 4), 75–131.
Wang, D., Hejazi, M., 2011. Quantifying the relative contribution of the climate and direct human impacts on mean annual streamflow in the contiguous United States. Water Resour. Res. 47 (10), 411.